Synthesis of thieno[3,2-*b*]thiophene derived conjugated oligomers for field-effect transistors applications

Weihua Tang,*[ab] Samarendra P. Singh,[a] Kok Haw Ong[a] and Zhi-Kuan Chen[a]

Received 28th September 2009, Accepted 25th November 2009
First published as an Advance Article on the web 4th January 2010
DOI: 10.1039/b920112b

A novel series of soluble thieno[3,2-*b*]thiophene (TT) oligomers with alternating TT and bithiophene or fluorene triad architectures have been synthesized for field-effect transistor (FET) applications. Their optical, thermal and electronic properties were investigated using UV-Vis and photoluminescence spectroscopy, thermal gravimetric analysis, and cyclic voltammetry. Compared with α,α′-dihexylsexithiophene (**D6HT**), these oligomers exhibit blue-shifted absorption spectra, 0.1 eV to 0.3 eV lower than the highest occupied molecular orbital (HOMO) energy levels and accordingly higher ambient stability. Their crystallinity and morphology features of these oligomers were further investigated with X-ray diffraction and atomic force microscopy using vacuum-deposited thin film on Si/SiO_2 substrate. Symmetrically structured TT-oligomers including **HT2TT**, **HTTT2**, **HTTTT** and **DDFTT** exhibit ordered film morphology and promising FET performance with devices fabricated by either vacuum deposition or solution processing techniques. Interestingly, **HTTT2** shows interconnected terrace island morphology, which is often observed for pentacene. All p-type transistors show promising performance, with **HT2TT** demonstrating a hole mobility up to 0.025 $cm^2V^{-1}s^{-1}$ and an on/off current ration $\sim 1.2 \times 10^3$ with vacuum sublimated film deposited on 70 °C substrate.

Introduction

Organic field-effect transistors (OFETs) based on either π-conjugated polymers or oligomers have generated great interest in both academic and industrial communities during the last decade.[1] Though OFETs still cannot rival the performance of single-crystalline inorganic counterparts, they do have the advantages of cost-effective manufacturing, simple processing and compatibility with plastic substrates, which offer them the potential in fabricating large-area devices with low cost.[1,2] In order to push OFETs to practical applications, the primary issues include the enhancement of their field-effect mobility (μ) to a level ($0.5\sim1$ $cm^2V^{-1}s^{-1}$), comparable to those of amorphous silicon-based thin film transistors.[1] Hence, it is crucial to develop high performance materials with facile synthesis protocols and controllable molecular packing and orientation, since the charge carriers' hopping between individual organic molecules strongly depend on the molecular arrangement.[2,3]

To date, a large spectrum of organic semiconductors such as oligoacenes,[4] and thiophenes and/or fused thiophene based oligomers[5] and polymers[6] has been explored as OFETs. Research efforts in oligoacenes have been inspired by the excellent performance of pentacene (mobilities up to 3.0 cm^2/Vs)[4e] and directed towards the development of chemically stable π-conjugated systems with planar shape facilitating crystal packing and extended conjugation over molecules.[7] Thiophene or fused thiophene, especially thieno[3,2-*b*]thiophene based conjugated systems have been developed as promising materials for OFETs due to their chemical stability, and versatile chemical modification to tune electronic properties.[5–7] Thieno[3,2-*b*]thiophene based polymers have demonstrated promising FET characteristics,[6] *e.g.* poly[2,5-bis(3-alkylthiophen-2-yl)-thieno[3,2-*b*]thiophene] showing a high mobility up to 0.6 $cm^2V^{-1}cm^{-1}$.[6c] However, the insufficient solubility of these polymers at room temperature makes it challenging for device fabrication through solution processing.[8] Compared with polymers, their oligomeric counterparts are advantageous in achieving good solution processability, facile synthesis and purification, well-defined structure design and even crystal packing.[2,9–11] Thiophene-based oligomers[12] are widely investigated due to their high mobility by taking advantage of the enhanced intermolecular ordering and π–π stacking.[13] However, a significant drawback of these p-channel semiconductors is their poor device stability due to the relatively low band gap and a high-energy highest occupied molecular orbital (HOMO) level, making them unsuitable for practical electronic circuit applications.[1d,14] For example, the model oligothiophene, α,α′-dihexyl-sexithiophene (**DH6T**, structure shown in Chart 1), shows an improved solubility, good hole mobility up to 0.5–1 $cm^2V^{-1}s^{-1}$ and an on/off ratio to 10^6, but a high HOMO ~-4.95, making it easily oxidized.[5e,9] To address this problem, design and synthesis of organic semiconductors with high charge carrier mobility as well as good stability is desirable. In our recent pursuit of polymer light-emitting diodes[15,16] and solar cells,[17] it is found thieno[3,2-*b*]-thiophene-based polyfluorene,[15] polycarbazole[16] and polyphenothiazines[17] exhibited excellent device stability and high charge transport properties due to their rigid structure and low HOMO levels.[15] In polyfluorene copolymers, the incorporation of thieno[3,2-*b*]thiophene (TT) instead of bithiophene (T2) was

[a]*Institute of Materials Research and Engineering, 3 Research Link, Singapore, 117602, Singapore. E-mail: whtang@mail.njust.edu.cn*
[b]*Nanjing University of Science and Technology, College of Chemistry and Chemical Engineering, Nanjing, 210094, People's Republic of China*

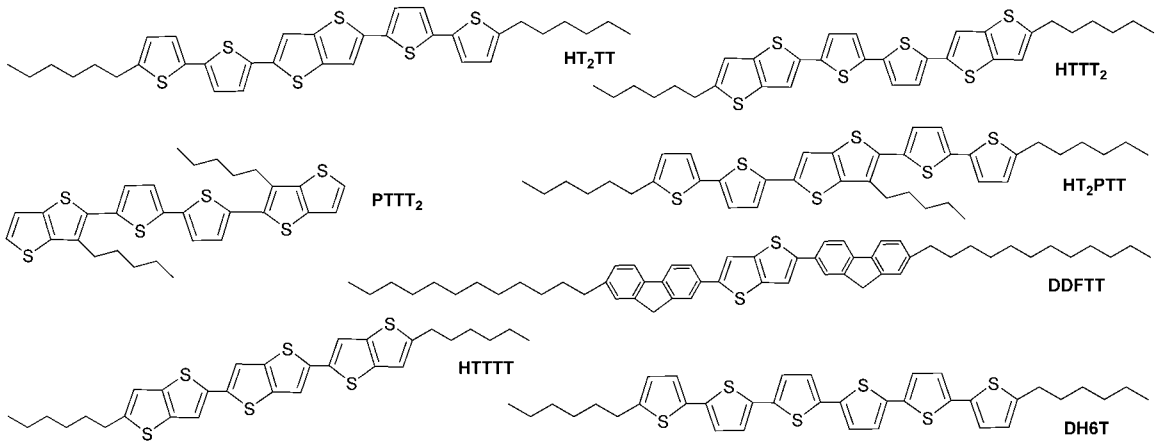

Chart 1

reported to endow the polymer with better FET characteristics.[6g] The objective of our present work is to develop straightforward protocols which allow up-scaling synthesis of thieno[3,2-*b*]thiophene oligomers with good solubility and ambient stability. For this purpose, six oligomers were end-capped with long alkyl chains while varied in the number of rigid structure of TT or fluorene (structures outlined in Chart 1).

Herein we report the synthesis and characterization of a series of new thieno[3,2-b]thiophene (TT) based oligomers. Except **PTTT2**, oligomers **HT2TT**, **HTTT2**, **HT2PTT**, **HTTTT** and **DDFTT** are all end-capped with long alkyl chain, which can improve the organic solvent-solubility and most importantly facilitate the self-assembly ability of the resulted oligomers.[5d,7e,8a,18] For comparison, **DH6T** was also synthesized as a reference molecule to evaluate the oxidation stability of our synthesized oligomers. These TT-oligomers were systematically characterized in terms of thermal properties, photophysical properties and electronic properties. Also their thin film crystallization and morphology were examined using X-ray diffraction (XRD) and atomic force microscopy (AFM). Finally, the preliminary FET characteristics were included and their promising potentials of these oligomers for OFET were elucidated.

Results and discussion

Synthesis

Scheme 1 outlines the synthetic approach for thieno[3,2-*b*]thiophene oligomers. The syntheses of **HT2TT** and **DDFTT** involved Suzuki coupling reaction between alkylated bithiophene or fluorene pinacolato boronic ester with the corresponding dibromo-substituted thieo[3,2-*b*]thiophene, while the synthesis of **HTTTT** and **HTTT2** involving the coupling reaction between 2-bromo-5-hexylthieno[3,2-*b*]thiophene **6** and disubstituted thieno[3,2-*b*]thiophene or bithiophene pinacolato boronic ester. The other two oligomers **PTTT2** and **HT2PTT** were synthesized by cross-coupling reactions between mono-pentylated thieno[3,2-*b*]thiophene and bithiophene building blocks. Thieno[3,2-*b*]thiophene **1** was prepared with the reported 4-step protocol.[19] Bromination of **1** with NBS affords the dibromo derivative **2**.[14–17] The boronic ester **3** was prepared by lithiation of **2** and followed borylation.[15–17] Mono α-alkylated thieno[3,2-*b*]thiophene **5** was achieved *via* Friedel–Crafts acylation and a further reduction of the resulted aldehyde **4** in a decent overall yield (*ca* 74%). This synthesis protocol overcomes the purification problems when directly conducting alkylation on **1** by reacting lithiated **1** with alkyl bromide.[11b] Mono-alkylated fluorene **11** was synthesized *via* Kumada coupling reaction using nickel(II) catalyst $[Ni(dppp)_2Cl_2]$. The synthesis of mono β-alkylated thieno[3,2-*b*]thiophene starts from a Friedel–Crafts acylation at the α position of 3-bromothiophene, followed by a ring closure reaction, hydrolysis and reduction.[15–17] The boronic ester of mono-alkylated fluorene **13** was achieved by Miyaura borylation with good yield (62%). With TT and fluorene building blocks (**2**, **3**, **6**, **8**, **10** and **13**) at hand, Suzuki cross-coupling technique was employed to prepare all TT-oligomers with satisfactory yields (52% to 76%). The newly synthesized TT-oligomers were structurally confirmed with NMR, mass analysis and elemental analysis. All oligomers are soluble in common organic solvents like toluene, THF, chloroform and 1,2-dichlorobenzene at room temperature.

The thermal stability of all oligomers was examined by thermal gravimetric analysis (TGA traces shown in Fig. 1). All oligomers exhibit good thermal stability as indicated by their decomposition temperature (T_d, temperature with 5% weight loss) over 200 °C. Generally, TT-oligomers have lower T_d when increasing the number of TT units. Therefore, **HTTTT** presents lower T_d (~268 °C) than **HTTT2** (313 °C), **DDFTT** (351 °C) and **PTTT2** (356 °C). When replacing of TT unit with T2 unit, **HT2TT** exhibits highest decomposition temperature (426 °C).

Electronic properties

The absorption spectra of all oligomers are plotted in Fig. 2, with the characteristic data including longest-wavelength absorptions (λ_{abs}^{max}) and onset-wavelength absorption (λ_{abs}^{onset}) summarized in Table 1. As clearly shown in Fig. 1 and Table 1, the λ_{abs}^{max} of TT-oligomers exhibits bathochromic-shifted spectra with an increase in their conjugation length. For oligomers **HT2TT**, **HTTT2** and **HTTTT**, the conjugation length decreases when bithiophene unit was gradually replaced by thieno[3,2-*b*]thiophene. Consequently, the λ_{abs}^{max} values of these oligomers decrease from 433 nm (**HT2TT**) to 417 nm (**HTTT2**) and 359 nm (**HTTTT**), suggesting that the 2,2′-bithiophene unit in **HT2TT** and **HTTT2** leads to a more

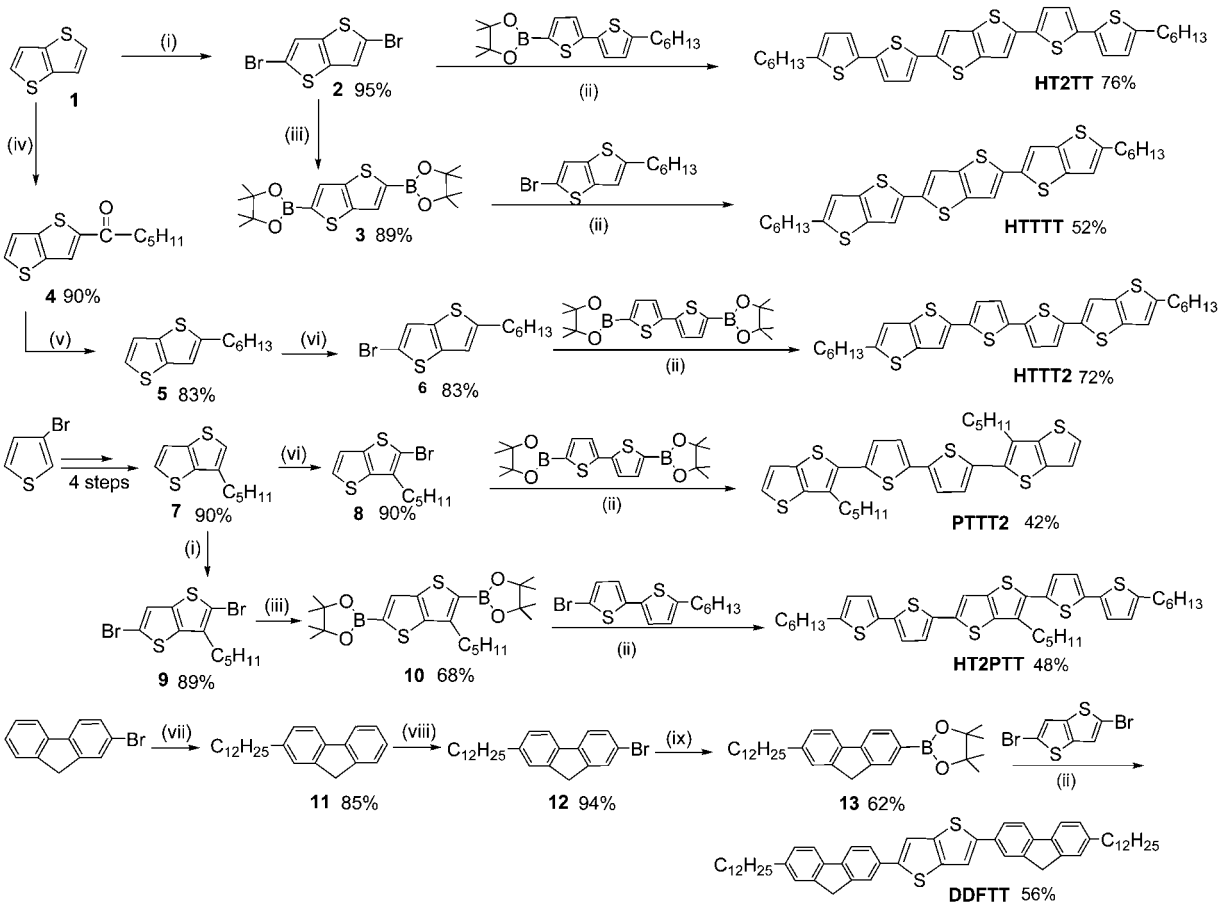

Scheme 1 Synthesis of solution-processable thien[3,2-b]thiophene-based oligomers *via* Suzuki coupling reaction. Reaction conditions: (i) 2 equivalent NBS, DMF, 0 °C, 3 h. (ii) $Pd(PPh_3)_4$, toluene/K_2CO_3 (2 M aqueous) = 2/3 (v/v), 80 °C, 24 h. (iii) *n*-BuLi, THF, −78 °C for 30 min before adding 2-isopropoxy-4,4,5,5-tetramethyl-1,3,2-dioxaborolane, −78 °C to room temperature, overnight. (iv) Hexanoyl chloride, $AlCl_3$, DCM. (v) $LiAlH_4$, $AlCl_3$, diethyl ether. (vi) 1 equivalent NBS, DMF, 0 °C, 3 h. (vii) $C_{12}H_{25}MgBr$, $Ni(dppp)_2Cl_2$, diethyl ether. (viii) NBS, propylene carbonate, 140 °C for 2 h, then leave to room temperature, overnight. (ix) bis(pinacolato)diboron, $Pd(dppf)_2Cl_2$, sodium acetate, DMSO, 80 °C, 16 h.

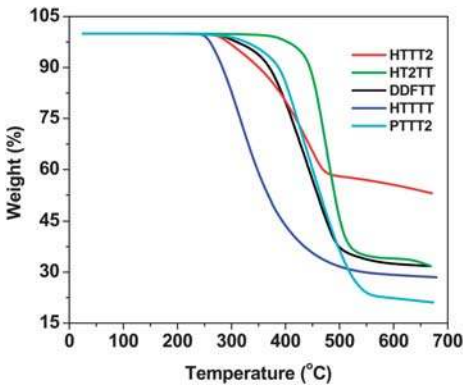

Fig. 1 TGA traces TT-oligomers measured under a nitrogen atmosphere.

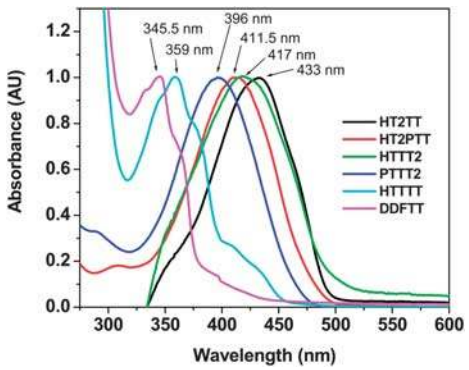

Fig. 2 UV-vis absorption spectra of TT-oligomers in THF solutions (~1 × 10^{-5} M).

conjugated oligomer than the corresponding thieno[3,2-*b*]thiophene unit in **HTTT2** and **HTTTT**. The similar behavior was also found in the polyfluorenes[15] and polythieno[3,2-*b*]thiophenes systems.[6f] Compared with **HT2TT**, **HT2PTT** shows a slightly blue-shifted λ_{abs}^{max}(411 nm) with the introduction of a β-substituted pentyl group, leading to less planar conformation.[6c] Similar trends can also be found when comparing the λ_{abs}^{max} values of **HTTT2** (417 nm) and **PTTT2** (396 nm), since a decreased planarity achieved in the latter when shifting the alkyl chain along the conjugated backbone as side chain.[6c] In comparison with **HTTTT**, **DDFTT** exhibits much blue-shifted absorption spectra due to the introduction of more rigid fluorene unit. The

Table 1 Observed longest-wavelength absorption (λ_{abs}^{max}), onset-wavelength absorption (λ_{abs}^{onset}), longest wavelength of fluorescence emission (λ_{PL}^{max}), HOMO and LUMO energy levels and band gaps determined from the optical and electrochemical measurements of the oligomers

oligomers	λ_{abs}^{max}/nm[a]	λ_{abs}^{onset}/nm	λ_{PL}^{max}/nm[a]	E_{ox}^{onset}/V	E_{red}^{onset}/V	HOMO/eV[b]	LUMO/eV[b]	E_g^{op}/eV[c]	E_g^{ec}/eV[b]
HT2TT	433	508	493.6 (525.7)	0.75	−1.73	−5.19	−2.71	2.44	2.48
HTTT2	417	494	489.3, 518.4	0.83	−1.69	−5.27	−2.75	2.51	2.52
PTTT2	396	473	489.5 (511.2)	0.64	−1.92	−5.08	−2.52	2.62	2.56
HT2PTT	411.5	479	503 (529.5)	0.72	−1.86	−5.16	−2.58	2.59	2.58
HTTTT	359	464	477.8 (467.7)	0.82	−1.78	−5.26	−2.66	2.67	2.60
DDFTT	345.5	445	440.2 (430.1)	0.85	−1.89	−5.29	−2.55	2.78	2.74
DH6T	409	511	505.5 (454.6)	0.55	−1.83	−4.99	−2.61	2.42	2.38

[a] 1×10^{-5} M in anhydrous THF solution, wavelength of maximum emission. The data in parentheses assigned for the wavelength of shoulder peak. [b] HOMO $= -|E_{ox}^{onset} + 4.4|eV$, LUMO $= -|E_{red}^{onset} + 4.4|eV$, E_g^{ec} = LUMO–HOMO. [c] optical band gap (E_g^{op}) calculated from onset value of the absorption spectrum in the long wavelength range (λ_{abs}^{onset}) according to the empirical equation ($E_g^{op} = 1240/\lambda_{abs}^{onset}$).

optical band gaps of these oligomers were determined from the optical onset value accordingly.[15–17] The optical band gaps of all oligomers range from 2.44 eV to 2.78 eV, with **DDFTT** exhibiting the widest band gap and **H2TTT2** the narrowest. The optical band gap decreases with increasing the conjugation length in the oligomer backbone.

The electronic states of the oligomers were investigated by cyclic voltammetry (CV) to understand the charge injection process and the stability of the oligomers. The onset oxidation potential (E_{ox}^{onset}) and onset reduction potential (E_{red}^{onset}) are listed in Table 1. The energy levels, *i.e.* the highest occupied molecular orbital (HOMO) levels and the lowest unoccupied molecular orbital (LUMO) levels, and electrochemical band gaps (E_g^{ec})[20] calculated from them are also summarized in Table 1. All oligomers showed partially reversible oxidation and reduction waves to afford radical cations and anions. All TT-oligomers exhibit a HOMO energy level in the range of −5.08 to −5.29 eV, which is 0.1 to 0.3 eV lower than that of **DH6T** (HOMO, −4.99 eV). The higher oxidation potential (lower HOMO level) achieved in these TT oligomers indicates their better oxidation stability than **DH6T**. The better oxidation stability can also be revealed by the higher E_g^{ec} values of TT oligomers (2.48∼2.74 eV) than that of **D6HT** (2.38 eV). The calculated E_g^{ec} values showed good agreement with the E_g^{op} values obtained from the onset absorption in UV-vis spectra. The determined HOMO level (−5.08∼−5.29 eV) matches well with the work function of gold, which facilitates the charge injection process from oligomer to gold electrode (source and drain electrodes) in FET devices.[21]

Crystallization and morphology study

It is generally accepted that the charge carrier transport in organic semiconductors is dominated through the hopping mechanism.[17c,22] Hence, it is necessary to achieve high ordered organic thin films with interconnected polycrystalline grains in order to obtain good performance OFETs.[7c] The ordered-structure and crystallization features of TT-oligomers were investigated by film X-ray diffraction (XRD) and atomic force microscopy (AFM). The XRD measurements in reflection mode were conducted on organic thin films deposited on 1,1,1,3,3,3-hexamethyldisilazane (HMDS) treated Si/SiO_2 substrate at room temperature. Generally, all symmetrically structured TT-oligomers including **HT2TT**, **HTTT2**, **HTTTT** and **DDFTT** showed high crystallinity, while oligomers **PTTT2** and **HT2PTT** only showed marginal crystallinity peaks. Fig. 3 shows the X-ray diffractograms of four symmetric TT-oligomers. The XRD patterns of the oligomer films exhibited high crystalline behavior with a strong primary diffraction peak at 2.96° for **HT2TT**, 3.17° for **HTTT2** and 3.03° for **DDFTT**, respectively. Interestingly, the dihexylated *tert*-thieno[3,2-b]thiophene, **HTTTT** exhibits a two-order diffraction pattern, with reflection peaks at 2.14° and 4.28°. These sharp peaks in the XRD spectra are attributed to the ordered interlayer stacking of the oligomer chains. Preferred orientation is clearly inferred through the dominance of peaks at 27∼41 Å. The spacing (27∼41 Å) corresponds exactly to the end-end packing length of molecular chains (*e.g.* **HT2TT**, 2θ of 2.96° corresponding to $d_{spacing} = 29.81$ Å).

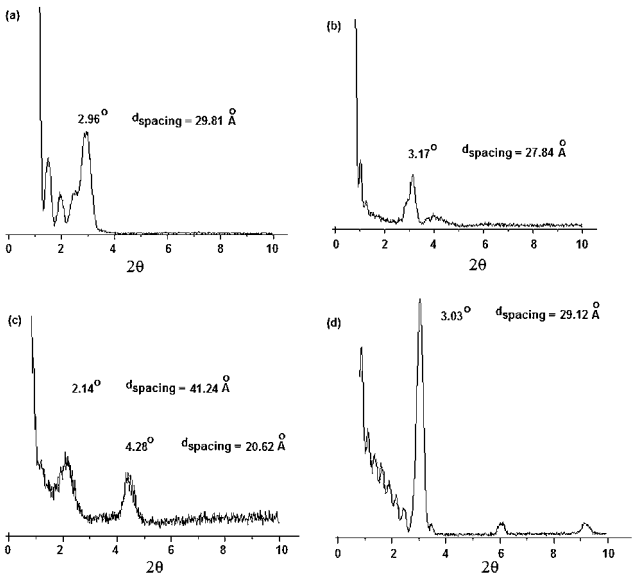

Fig. 3 X-ray reflection diagrams of **HT2TT** (a), **HTTT2** (b), **HTTTT** (c) and **DDFTT** (d) thin films on HMDS/Si/SiO_2 substrate at 25 °C.

The AFM topographic images of **HT2TT** and **HTTTT** on HMDS-treated Si/SiO_2 substrate are shown in Fig. 4, while the thin film morphologies of **DDFTT** and **HTTT2** are displayed in Fig. 5. Highly ordered thin-film structures are formed for all four oligomers. As shown in Fig. 4, films of **HTTTT** show homogenous morphology with small rod-like features (ca 100 nm in diameter) and a surface roughness ∼45 nm. However, **HT2TT**

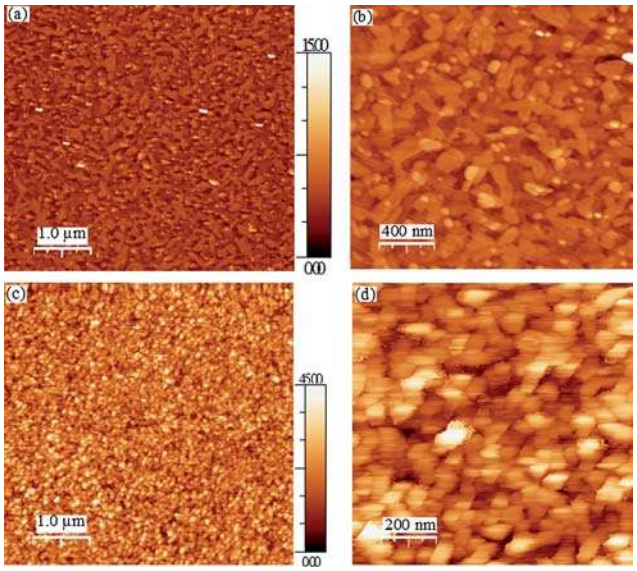

Fig. 4 AFM Images of **HT2TT** (a, b) and **HTTTT** (c, d) thin films (thickness ~35 nm) on HMDS/Si/SiO_2 substrate at room temperature.

film shows a heterogeneous morphology with lower surface roughness (~15 nm) and hybrid granule-rod feature, in which the rod-like features show larger dimension range (100 nm~200 nm). A close look at the morphology of **DDFTT** film, it features a homogenous rod-like morphology with a surface roughness ~50 nm. The rod-like features of **DDFTT** show average dimension of 200 nm in length (Fig. 5, top panel). The film morphology of **HTTT2** shows the most favorable terrace feature and each terrace is associated with up to the fourth and sixth layer. This attractive morphology is very similar to that of pentacene[4,23] and fluroene-thiophene oligomer[10b] grown under the typical growth conditions used here, contributed for the highest reported OFET mobility. The growth scenario of **HTTT2** may be described as crystallites initially grown in a quasi layer-by-layer mode and then changes to a rapid growth of several layers (3D growth) as the coverage increases due to kinetic processes.[23] Top layers of the terrace appear white in the topographical image (Fig. 5, bottom panel) due to its larger height (~20 nm) in comparison to the step height of the **HTTT2** monomolecular layer (~1.5 nm). Despite the difference in the morphology features of four oligomers, we have full covering of substrate with ordered topographic features and good network interconnection between adjacent lamellas, which is favorable for high charge-carrier mobility in OFETs.

FET performance

All FET devices were made in top contact geometry with solution processing technique,[24] while the fabrication of **HT2TT** devices was explored with vacuum deposition and the effect of substrate temperature was examined. The FET characteristic data for **HT2TT**, **DDFTT**, **HTTTT** and **HTTT2** are summarized in Table 2. All devices exhibit p-channel performance with the mobility calculated from the saturation regime. Fig. 6 shows the typical current–voltage characteristics of **HT2TT** device made by vacuum deposition at room temperature on HMDS-treated Si/SiO_2 substrate. This device demonstrates a saturation hole mobility of 1.1×10^{-2} $cm^2V^{-1}s^{-1}$ and an on/off ratio of 1.2×10^3. When vacuum deposition of **HT2TT** on 70 °C substrate to improve better molecular ordering, the device shows a highest hole mobility up to 2.5×10^{-2} $cm^2V^{-1}s^{-1}$ and on/off current ration ~1.2×10^3. As shown in Table 2, by spin-coating oligomer solution in toluene, **DDFTT** shows good FET performance with a high mobility of 1.7×10^{-2} $cm^2V^{-1}s^{-1}$ and on/off current ratio of 4.2×10^3. This device performance is very promising as compared to other solution processed thiophene-based FETs.[24] Solution-processed devices for **HTTTT** and **HTTT2** also demonstrate promising FET characteristics with mobility up to 1.6×10^{-3} and 3.1×10^{-3} $cm^2V^{-1}s^{-1}$, and on/off ratios of 3.1×10^2 and 2.6×10^2, respectively. In addition, the **DDFTT** and **HTTTT** devices showed good threshold voltages of −25 V and −36 V, respectively. The vacuum-deposited FETs devices are still under optimization with surface modification, substrate temperature and device geometry. Their device performance will be reported later. In summary, symmetric TT-oligomers are promising materials for OFET.

Table 2 Observed longest-wavelength absorption (λ_{abs}^{max}), onset-wavelength absorption (λ_{abs}^{onset}), longest wavelength of fluorescence emission (λ_{PL}^{max}), HOMO and LUMO energy levels and band gaps determined from the optical and electrochemical measurements of the oligomers

Oligomers	$\mu/cm^2V^{-1}s^{-1}$	V_{TH}/V	On/off ratio
HT2TT (sublimation rt)[c]	1.1×10^{-2}	−4.2	1.2×10^3
HT2TT (sublimation 70 °C)[c]	2.5×10^{-2}	−4.0	1.2×10^3
HTTTT (solution processing)	1.6×10^{-3}	−36	3.1×10^2
HTTT2 (solution processing)	3.1×10^{-3}	−5.5	2.6×10^2
DDFTT (solution processing)	1.7×10^{-2}	−25	4.2×10^3

[a] Mobility is calculated using currents from saturation regions. [b] On/off ratios is calculated for gate voltages from 0 to −70 V. [c] Vacuum deposition.

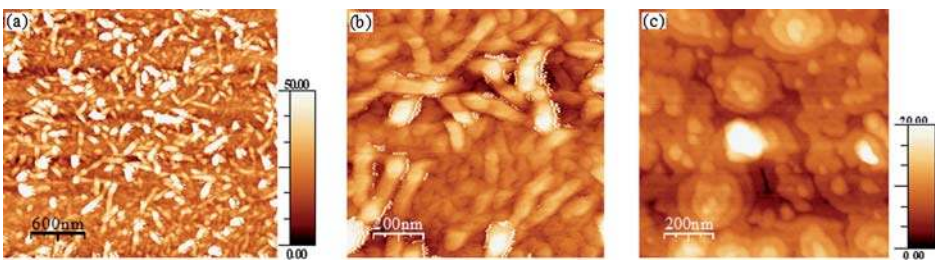

Fig. 5 AFM Images of **DDFTT** (a, b) thin films (thickness ~20 nm) and **HTTT2** (c) thin films (thickness ~35 nm) on HMDS/Si/SiO_2 substrate at room temperature.

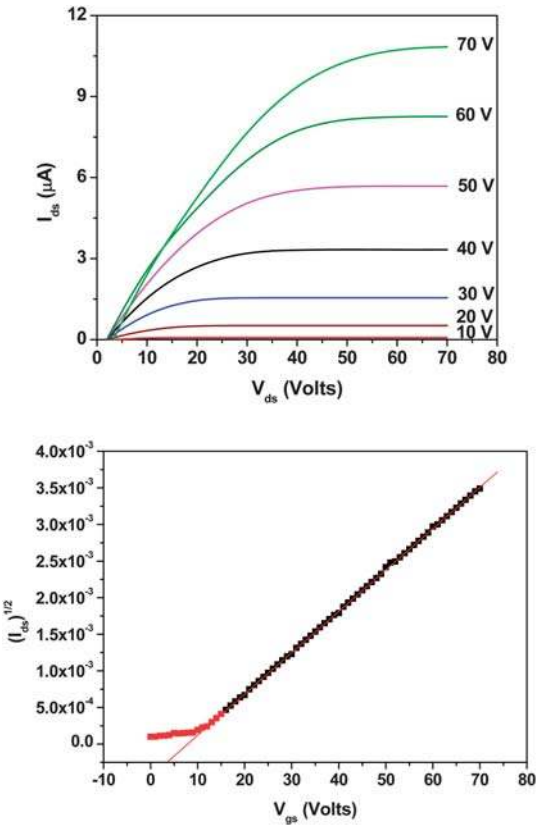

Fig. 6 Current–voltage (top) $I_{ds} - V_{ds}$, and (bottom) $I_{ds} - V_{gs}$ characteristic of **HT2TT** on HMDS/Si/SiO_2 substrate.

Conclusions

A novel series of thieno[3,2-*b*]thiophene-based solution-processable oligomers with alkylated thiophene or fluorene functionality as terminal group have been synthesized by using Suzuki cross-coupling reaction as the key step. All TT-oligomers exhibit advantages such as higher thermal and good solubility over oligothiophenes. They should also possess higher oxidation stability as indicated by their low HOMO levels. In UV-vis absorption spectra, the maximum absorption of these oligomers showed bathochromic shifts with increasing conjugation length. Their HOMO levels ranging from −5.08 to −5.29 eV match well with the work function of gold, facilitating smooth charge injection process in FET devices. XRD investigations reveal that symmetric TT-oligomers including **HT2TT**, **HTTT2**, **HTTTT** and **DDFTT** are crystalline in nature, with reasonable lamellar spacing ($d_{spacing}$). The ordered thin-film morphology was clearly observed in AFM images. Interconnected rod-like or terrace island patterns fully covered the substrate, which is favorable for high charge-carrier mobility. The FET performance of these oligomers was examined by fabrication of devices by either solution processing or vacuum deposition technique. Among them, **HT2TT** showed relatively good FET characteristics with mobility up to 2.5×10^{-2} $cm^2V^{-1}s^{-1}$ and on/off current ratios of $\sim 1.2 \times 10^3$. Solution-processed FETs with **DDFTT** and **HTTTT** exhibited a promising mobility of 1.7×10^{-2} $cm^2V^{-1}s^{-1}$ and 1.6×10^{-3} $cm^2V^{-1}s^{-1}$, respectively. The device performance can be further improved by optimizing different processing conditions. The results of the present study would be helpful in the future design of more effective TT-based FETs.

Experimental section

Instrumentation

^1H NMR and ^{13}C NMR spectra were recorded on a Bruker 400 MHz DPX FT-NMR spectrometer. Matrix assisted laser desorption/ionization time-of-flight (MALDI-TOF) mass spectra were obtained on a Bruker Autoflex TOF/TOF instrument using dithranol as the matrix. The UV-vis absorption and photoluminescence (PL) spectra were recorded on a Shimadzu UV 3101 spectrophotometer and on a Perkin-Elmer LS-50B luminescence spectrometer, respectively. Thermal gravimetric analysis (TGA) was performed at a heating rate of 20 °C min^{-1} under N_2 atmosphere with DuPont TGA 2050. Cyclic voltammetry (CV) measurements were performed on AUTOLAB work station (model PGSTAT30) with 0.10 M Bu_4NBF_4 dichloromethane solution (scan rate, 100 mV s^{-1}) as electrolyte. Three electrodes including a platinum plate working electrode, a copper counter electrode, and a Ag/AgCl in 3 M KCl reference electrode were used.

FET fabrication and characterization

Thin-film field-effect transistors were fabricated in glovebox under N_2 on highly n-doped Si substrates (gate electrode) with 200 nm of thermally grown SiO_2 (insulating layer) in top contact configuration. FET substrates were treated with HMDS. Thin films of oligomers, typically 20, 30 or 35 nm, were deposited using vacuum sublimation (at a rate of 0.5–1.0 Å s^{-1} under a pressure of 7×10^{-6} mbar) or spin-coated onto HMDS-treated substrate. Transistor source and drain gold electrodes (~100 nm) were deposited on a SiO_2 layer through a shadow mask to offer OFET devices with a channel length of 200 μm and channel width of 6 mm. The FET characterization was performed on a computer-controlled Keithley 4200 parameter analyzer and all measurements were conducted at room temperature under nitrogen. From the electrical transfer characteristics (I_d-V_g), the parameters including carrier mobility, threshold voltage and current on/off ration were extracted. The carrier mobility (μ) was calculated in the saturation regime and current on/off ratio was calculated from the I_{ds} as previously.[24]

XRD and AFM characterization

Thin films of oligomer samples were vacuum deposited on HMDS/Si/SiO_2 substrate at room temperature for both characterizations. X-ray diffraction studies were performed on PANalytical X'PERT PRO system using Cu-Kα source in air. Molecular Imaging Veeco Metrology Digital Instruments microscope was used to perform tapping mode AFM (AP-0195, Park Scientific Instruments) on samples with a silicon tip of 300 kHz frequency.[24]

Synthesis

All starting materials and reagents were purchased from Sigma-Aldrich Chemical Co. and used without further purification.

THF was dried over sodium/benzophenone and freshly distilled before use. Thieno[3,2-b-]thiophene (**1**), 2,5-dibromo-thieno-[3,2-*b*]thiophene (**2**), 3-pentylthieno[3,2-*b*]thiophene (**7**), and 2,5-dibromo-3-pentylthieno[3,2-*b*]thiophene, (**9**) were prepared according to the reported procedures.[15–17,19]

2,5-Bis(4,4,5,5-tetramethyl-1,3,2-dioxaborolan-2-yl)-thieno[3,2-*b*-]thiophene (3). To a solution of **2** (4.17 g, 13.95 mmol) in THF (100 mL) at −78 °C was charged with 1.4 M n-butyllithium hexane solution (24.91 mL, 34.87 mmol) of). The mixture was stirred at −78 °C for 30 min. 2-Isopropoxy-4,4,5,5-tetramethyl-1,3,2-dioxaborolane (6.5 g, 34.87 mmol) was added rapidly to the solution and left the reaction overnight at room temperature. The reaction was deactivated by water and the reaction mixture was extracted with ether. The organic extracts were washed with brine and dried over anhydrous $MgSO_4$. After removal of organic solvent, the residue was purified by silica gel column chromatography (ethyl acetate–hexane = 1 : 20) and recrystallized from hexane to afford the *title* compound as a grey solid (4.87 g, 89%). ^{1}H NMR (400 MHz, $CDCl_3$): δ (ppm) 7.76 (s, 2H), 1.36 (s, 24H). MALDI-TOF-MS: *m/z* = 392.53 (M); calcd for $C_{18}H_{26}B_2O_4S_2$ = 392.15.

2-Hexanoylthieno[3,2-*b*-]thiophene (4). Hexanoyl chloride (2.07 g, 15.4 mol) was added into a solution of **1** (1.40 g, 10 mmol) in CH_2Cl_2 (20 mL). $AlCl_3$ (2.0 g, 15 mmol) was added in portions over 30 min. The mixture was stirred for 1 h at room temperature. The reaction mixture was then poured into ice water and extracted with CH_2Cl_2 (3 × 20 mL). The organic phase was washed with 2 M HCl and brine and dried over $MgSO_4$. After removal of the solvent, the residue was recrystallized from ethanol to afford the *title* compound as a white solid (1.72 g, 72%). ^{1}H NMR (400 MHz, $CDCl_3$): δ (ppm) 7.90 (s, 1H), 7.61 (d, *J* = 4.2 Hz, 1H), 7.29 (d, *J* = 4.2 Hz, 1H), 2.92 (t, *J* = 7.6 Hz, 2H), 1.78 (tt, *J* = 7.6 Hz, *J* = 7.2 Hz, 2H), 1.40 − 1.35 (m, 4H), 0.92 (t, *J* = 6.8 Hz, 3H). ^{13}C NMR (100 MHz, $CDCl_3$): δ (ppm) 146.43, 145.12, 139.51, 132.66, 124.43, 120.44, 39.45, 31.93, 29.07, 25.05, 22.86, 14.29. MALDI-TOF-MS: *m/z* = 238.14 (M); calcd for $C_{12}H_{14}OS_2$ = 238.37.

2-Hexylthieno[3,2-*b*-]thiophene (5). 2-Hexanoylthieno[3,2-*b*] thiophene (0.95 g, 4 mmol) was dissolved in freshly distilled THF (10 mL). This solution was then added to a suspension of $LiAlH_4$ (1.24 g, 32.6 mmol) and $AlCl_3$ (1.09 g, 8.2 mmol) in anhydrous ether (20 mL) under N_2 at 0 °C. After warming to room temperature, the reaction was quenched by successively adding ethyl acetate (10 mL) and aqueous HCl solution (6 M, 10 mL). The organic phase was separated and the aqueous phase was extracted with ether. The combined organic phases were dried over $MgSO_4$ and evaporated *in vacuo*. The crude product was subject to silica gel column chromatography (eluent, hexane) to afford a colorless oil (0.74 g, 83%). ^{1}H NMR (400 MHz, $CDCl_3$): δ (ppm) 7.28 (d, *J* = 4.2 Hz, 1H), 7.18 (d, *J* = 4.2 Hz, 1H), 6.96(s, 1H), 2.88 (t, *J* = 7.2 Hz, 2H), 1.73 (tt, *J* = 7.6 Hz, *J* = 7.2 Hz, 2H), 1.42 − 1.28 (m, 6H), 0.93 (t, *J* = 6.8 Hz, 3H). ^{13}C NMR (100 MHz, $CDCl_3$): δ (ppm) 148.99, 139.21, 137.77, 125.60, 119.81, 116.53, 31.97, 31.92, 29.14, 22.95, 14.41. MALDI-TOF- MS: *m/z* = 224.20 (M); calcd for $C_{12}H_{16}S_2$ = 224.38.

2-Bromo-5-hexylthieno[3,2-*b*-]thiophene (6). To a solution of **3** (1.8 g, 8.0 mmol) in DMF (10 mL) at 0 °C was charged with a solution of NBS (1.5 g, 8.4 mmol) in DMF (10 mL). After 3 h stirring at 0 °C, crushed ice was added and the mixture solution was extracted with CH_2Cl_2 (3 × 20 mL). The combined organic layers were washed with water (3 × 100 mL) and dried over anhydrous $MgSO_4$. After solvent removal in *vacuo*, the residue was subjected to silica gel column chromatography (eluent, hexane). The *title* product was obtained as a white solid (2.06 g, 85%). ^{1}H NMR (400 MHz, $CDCl_3$): δ (ppm) 7.17 (s, 1H), 6.85(s, 1H), 2.84 (t, *J* = 7.2 Hz, 2H), 1.69 (tt, *J* = 7.6 Hz, *J* = 7.2 Hz, 2H), 1.39−1.25 (m, 6H), 0.89 (t, *J* = 6.8 Hz, 3H). MALDI-TOF-MS: *m/z* = 303.19 (M); calcd for $C_{12}H_{15}$ Br S_2 = 303.28.

2-Bromo-3-pentylthieno[3,2-*b*]thiophene (8). Following the similar synthetic approach as for **6**, the *title* compound was obtained as a white solid (yield, 90%). ^{1}H NMR (400 MHz, $CDCl_3$): δ (ppm) 7.37 (d, *J* = 5.2 Hz, 1H), 7.15 (d, *J* = 5.2 Hz, 2H), 2.72 (t, *J* = 7.6 Hz, 2H), 1.76 − 1.68 (tt, *J* = 7.6 Hz, 6.8 Hz, 2H), 1.22 − 1.27 (br, 4H), 0.89 (t, *J* = 6.8 Hz, 3H). ^{13}C NMR (100 MHz, $CDCl_3$): δ (ppm) 140.43, 139.18, 135.30, 127.25, 122.12, 120.30, 31.97, 30.35, 28.73, 22.85, 14.48. MALDI-TOF-MS: *m/z* = 289.13 (M); calcd for $C_{11}H_{13}Br$ S_2 = 289.25.

2,5-bis(4,4,5,5-tetramethyl-1,3,2-dioxaborolan-2-yl)-3-pentyl-thieno[3,2-*b*-]thiophene (10). By following the similar approach as for **3**, 2.5 equivalent n-butyllithium and 2-isopropoxy-4,4,5,5-tetramethyl-1,3,2-dioxaborolane were used in the synthesis. The final product was purified through column chromatography (ethyl acetate–hexane = 1 : 20) and recrystallized from hexane to give the analytically pure *title* compound as a grey solid (4.51 g, 68%). ^{1}H NMR (400 MHz, $CDCl_3$): δ (ppm) 7.72 (s, 1H), 3.02 (t, *J* = 7.6 Hz, 2H), 1.74 − 1.70 (t, *J* = 6.8 Hz, 2H), 1.24 − 1.37 (br, 30H), 0.88 (t, *J* = 6.8 Hz, 3H). MALDI-TOF- MS: *m/z* = 462.01 (M); calcd for $C_{23}H_{36}B_2O_4S_2$ = 462.28.

2,5-Bis(5-hexyl-2,2′-bithiophen-2-yl)-thieno[3,2-*b*]thiophene (HT2TT). To a solution of **2** (0.12 g, 0.4 mmol) and 5-(5′-hexyl-2,2′-bithiophene-2-yl)-4,4,5,5-tetramethyl-1,3,2-dioxaborolane (0.39 g, 1.04 mmol) dissolved in toluene (5 mL) was added 2 M potassium carbonate aqueous solution (3 mL). The mixture was degassed for 30 min and then $Pd(PPh_3)_4$ (55 mg, 0.048 mmol) was added. The mixture was heated to 85 °C for 48 h under N_2. After cooling down to room temperature, the reaction mixture was poured into methanol (100 mL). The precipitate was filtered off, washed with water, dilute HCl solution (5%) and water. The crude product was purified by Soxhlet extraction in acetone and methanol each for 1 day to give an orange yellow powder (yield, 76%). ^{1}H NMR (400 MHz, $CDCl_3$): δ (ppm) 7.02 (d, *J* = 5.2 Hz, 2H), 6.99 (s, 2H), 6.98 − 6.96 (m, 4H), 6.68 (d, *J* = 5.2 Hz, 2H), 2.79 (t, *J* = 7.6 Hz, 4H), 1.68 (tt, *J* = 7.2 Hz, *J* = 6.8 Hz, 4H), 1.43 − 1.24 (m, 12H), 0.89 (t, *J* = 7.6 Hz, 6H). MALDI-TOF-MS: *m/z* = 637.29 (M); calcd for $C_{34}H_{36}S_6$ = 637.04. Elemental Anal. Found: C, 66.93; H, 6.88; S, 29.97. Calcd: C, 64.10; H, 5.70; S, 30.20.

2,5-Bis(5-hexyl-2,2′-bithiophen-2-yl)-3-pentylthieno[3,2-*b*]thiophene (HT2PTT). Following the similar synthetic method as for **HBTTT**, Suzuki coupling of **9** and 5-(5′-hexyl-2,2′-bithiophene-2-yl)-4,4,5,5-tetramethyl-1,3,2-dioxaborolane afforded the *title*

compound as a deep red powder (yield, 48%). ^{1}H NMR (400 MHz, $CDCl_3$): δ (ppm) 7.09 (d, $J = 6.0$ Hz, 2H), 7.07 – 6.97 (m, 6H), 6.70 (s, 1H), 2.91 (t, $J = 7.6$ Hz, 2H), 2.79 (t, $J = 7.6$ Hz, 4H), 1.77 (tt, $J = 7.2$ Hz, $J = 6.8$ Hz, 2H), 1.67 (tt, $J = 7.2$ Hz, $J = 6.8$ Hz, 4H), 1.43 – 1.24 (m, 16H), 0.88 (t, $J = 7.6$ Hz, 9H). ^{13}C NMR (100 MHz, $CDCl_3$): δ (ppm) 146.45, 143,82, 138.71, 135.56, 132.02, 127.09, 125.23, 125.04, 123.99, 123.62, 116.43, 32.21, 31.87, 30.58, 29.38, 29.11, 22.90, 14.35. MALDI-TOF-MS: m/z = 707.32 (M); calcd for $C_{39}H_{46}S_6$ = 707.17. Elemental Anal. Found: C, 66.93; H, 6.88; S, 27.04. Calcd: C, 66.24; H, 6.56; S, 27.21.

5,5′-Bis(5-hexyl-thieno[3,2-*b*]thiophen-2-yl)-2,2′-bithiophene (HTTT2). Suzuki coupling of **10** and 5-bromo-5′-hexyl-2,2′-bithiophene afforded an orange-red powder (yield, 72%). ^{1}H NMR (400 MHz, $CDCl_3$): δ (ppm) 7.22 (d, $J = 5.2$ Hz, 2H), 7.18 (d, $J = 5.2$ Hz, 2H), 7.08 (s, 2H), 6.91 (s, 2H), 2.87 (t, $J = 7.6$ Hz, 4H), 1.72 (tt, $J = 7.6$ Hz, $J = 7.2$ Hz, 4H), 1.45 – 1.32 (m, 12H), 0.88 (t, $J = 7.6$ Hz, 6H). MALDI-TOF-MS: m/z = 612.24 (M); calcd for $C_{32}H_{34}S_6$ = 611.00. Elemental Anal. Found: C, 62.76; H, 5.92; S, 32.08. Calcd: C, 62.90; H, 5.61; S, 31.49.

5,5′-Bis(3-pentyl-thieno[3,2-*b*]thiophen-2-yl)-2,2′-bithiophene (PTTT2). Suzuki coupling of **8** and 5-(5′-hexyl-2,2′-bithiophene-2-yl)-4,4,5,5-tetramethyl-1,3,2-dioxaborolane afforded a deep red powder (yield, 42%). ^{1}H NMR (400 MHz, $CDCl_3$): δ (ppm) 7.37 (d, $J = 5.2$ Hz, 2H), 7.23 (d, $J = 5.2$ Hz, 2H), 7.17 (d, $J = 3.6$ Hz, 2H), 7.08 (d, $J = 3.6$ Hz, 2H), 2.95 (t, $J = 8.0$ Hz, 4H), 1.80 (tt, $J = 7.2$ Hz, $J = 6.8$ Hz, 4H), 1.47 – 1.34 (m, 12H), 0.88 (t, $J = 7.6$ Hz, 6H). ^{13}C NMR (100 MHz, $CDCl_3$): δ (ppm) 145,53, 141.81, 137.53, 136.78, 136.14, 132.28, 127.24, 126.99, 124.25, 120.05, 32.20, 29.40, 28.90, 22.76, 14.20. MALDI-TOF-MS: m/z = 582.84 (M); calcd for $C_{30}H_{30}S_6$ = 582.95. Elemental Anal. Found: C, 61.93; H, 5.35; S, 32.88. Calcd: C, 61.81; H, 5.19; S, 33.00.

2,5-Bis(5-hexyl-thieno[3,2-*b*]thiophen-2-yl)-thio[3,2-b]thiophene (HTTTT). Suzuki coupling of **3** and **6** afforded an orange red powder (yield, 52%). ^{1}H NMR (400 MHz, $CDCl_3$): δ (ppm) 7.34 (s, 2H), 7.30 (s, 2H), 6.92 (s, 2H), 2.88 (t, $J = 7.6$ Hz, 4H), 1.72 (tt, $J = 7.6$ Hz, $J = 7.2$ Hz, 4H), 1.43 – 1.21 (m, 12H), 0.90 (t, $J = 7.6$ Hz, 6H). MALDI-TOF-MS: m/z = 584.82 (M); calcd for $C_{30}H_{32}S_6$ = 584.96. Elemental Anal. Found: C, 61.92; H, 5.69; S, 32.45. Calcd: C, 61.60; H, 5.51; S, 32.89.

2-Dodecyl-9*H*-fluorene (11). Treatment of n-dodecyl bromide (14.95 g, 60 mmol) with Mg (1.44 g, 60 mmol) in ether (100 mL), a Grignard reagent of n-dodecylmagnesium bromide was prepared and added dropwise into a solution of 2-bromo-9*H*-fluorene (12.26 g, 50 mmol) and Ni(dppp)$_2$Cl$_2$ (0.25 g, 4 mmol) in ether over 1 h. After refluxing 20 h, the reaction mixture was cooled down to room temperature and quenched with 0.2 M HCl solution. The resultant mixture was extracted with ether and washed with water (3 × 50 mL), followed with brine and dried over anhydrous $MgSO_4$. Evaporation of solvent afforded a white powder, which was further purified by silica gel column chromatography (eluent, hexane). Recrystalization from methanol afforded the *title* compound as a white crystal (14.25 g, 85%). ^{1}H NMR (400 MHz, $CDCl_3$): δ (ppm) 7.75 (d, $J = 7.6$ Hz, 1 H), 7.69 (d, $J = 8.0$ Hz, 1 H), 7.52 (d, $J = 7.6$ Hz, 1 H), 7.36 – 7.35 (m, 1 H), 7.33 (s, 1 H), 7.28 – 7.24 (m, 1H), 7.19 (d, $J = 7.6$ Hz, 1H), 3.87 (s, 2H), 2.67 (t, $J = 7.6$ Hz, 2 H), 1.67 – 1.62 (m, 2 H), 1.38 – 1.25 (m, 18 H), 0.88 (t, $J = 6.8$ Hz, 3 H). MALDI-TOF-MS: m/z = 334.58 (M); calcd for $C_{25}H_{34}$ = 334.54.

2-Bromo-7-dodecyl-9*H*-fluorene (12). A mixture solution of 2-dodecyl-9*H*-fluorene (5.01 g, 15 mmol) and NBS (2.67 g, 15 mmol) in propylene carbonate (50 mL) was heated at 140 °C for 2 h. The reaction mixture was then poured into water (100 mL). After filtration and washing with water, the precipitate was further purified by silica gel column chromatography with hexane as eluent. Removal of solvent resulted in a light yellow powder (5.84 g, 94%). ^{1}H NMR (400 MHz, $CDCl_3$): δ (ppm) 7.65 (d, $J = 7.6$ Hz, 1H), 7.64 (s, 1H), 7.59 (d, $J = 7.6$ Hz, 1H), 7.47 (d, $J = 7.6$ Hz, 1H), 7.35 (s, 1H), 7.19 (d, $J = 7.6$ Hz, 1H), 3.85(s, 2H), 2.67 (t, $J = 7.6$ Hz, 2H), 1.68 – 1.61 (m, 2H), 1.35 – 1.24 (m, 18H), 0.88 (t, $J = 6.8$ Hz, 3H). ^{13}C NMR (100 MHz, $CDCl_3$): δ (ppm) 145.51, 143.49, 142.77, 141.26, 138.72, 130.19, 128.57, 127.67, 125.48, 121.17, 120.28, 120.06, 37.05, 36.56, 32.31, 32.14, 30.05, 29.92, 29.73, 23.03, 14.48. MALDI-TOF-MS: m/z = 413.62; calcd for $C_{25}H_{33}Br$ = 413.43.

2-(7-dodecyl-9*H*-fluoren-2-yl)-4,4,5,5-tetramethyl-1,3,2-dioxaborolane (13). A standard Miyaura borylation was used. To a 100 mL one-necked flask was charged with **12** (2.07 g, 5 mmol), bis(pinacolato)diboron (1.40 g, 5.5 mmol), and Pd(dppf)$_2$Cl$_2$ complex with dichloromethane (1 : 1) (0.13 g, 0.16 mmol). Anhydrous DMSO (40 mL) was then added and the mixture was degassed with N_2 for 30 min. The reaction solution was heated at 80 °C for 16 h and then cooled down to room temperature. The reaction mixture was poured into ice water (200 mL). Extracted with ether (3 × 20 mL) and dried over $MgSO_4$, the organic phase was evaporated and the residue was further purified by silica gel column chromatography (dichloromethane–hexane = 1 : 2) as eluent to afford the *title* compound as a white solid (1.43 g, 62%). ^{1}H NMR (400 MHz, $CDCl_3$): δ (ppm) 7.96 (s, 1H), 7.82 (d, $J = 7.6$ Hz, 1H), 7.74 (d, $J = 7.6$ Hz, 1H), 7.68 (d, $J = 7.6$ Hz, 1H), 7.36 (s, 1H), 7.18 (d, $J = 7.6$ Hz, 1H), 3.85(s, 2H), 2.67 (t, $J = 7.6$ Hz, 2H), 1.67 – 1.61 (m, 2H), 1.35 – 1.22 (m, 30H), 0.87 (t, $J = 7.6$ Hz, 3H). MALDI-TOF-MS: m/z = 460.37 (M); calcd for $C_{31}H_{45}BO_2$ = 460.50. Elemental Anal. Found: C, 81.74; H, 9.98; B, 2.18. Calcd: C, 80.85; H, 9.85; B, 2.35.

2,5-Bis(7-dodecyl-9*H*-fluoren2-yl)-thieno[3,2-b]thiophene (DDFTT). Suzuki coupling of **2** and **13** afforded a light yellow powder (yield, 56%). ^{1}H NMR (400 MHz, $CDCl_3$): δ (ppm) 7.78 (s, 2H), 7.74 (d, $J = 8.0$ Hz, 2H), 7.69 (d, $J = 8.0$ Hz, 2H), 7.64 (d, $J = 8.0$ Hz, 2H), 7.52 (s, 2H), 7.38 (s, 2H), 7.20 (d, $J = 8.0$ Hz, 2H), 3.92(s, 4H), 2.68 (t, $J = 7.6$ Hz, 4H), 1.67 – 1.60 (m, 4H), 1.36 – 1.21 (m, 36H), 0.88 (t, $J = 7.6$ Hz, 6H). ^{13}C NMR (100 MHz, $CDCl_3$): δ (ppm) 144.36, 144.08, 142.55, 142.36, 133.29, 127.61, 126.90, 125.48, 125.14, 122.79, 120.30, 120.07, 119.98, 115.29, 37.22, 36.57, 32.29, 32.11, 30.02, 29.91, 29.73, 23.03, 14.42. MALDI-TOF-MS: m/z = 805.17(M); calcd for $C_{56}H_{68}S_2$ = 805.27. Elemental Anal. Found: C, 82.47; H, 8.36; S, 7.74. Calcd: C, 83.52; H, 8.51; S, 7.96.

References

1 (*a*) M. Muccini, *Nat. Mater.*, 2006, **5**, 605; (*b*) H. Sirringhaus, L. Buergi, T. Kawase and R. H. Friend, in *Thin Film Transistors* (Eds: C. R. Kagan, P. Andry), Marcel Dekker, New York 2003, p. 427; (*c*) S. R. Forrest, *Nature*, 2004, **428**, 911; (*d*) H. Sirringhaus, *Adv. Mater.*, 2005, **17**, 2411; (*e*) H. E. Katz, Z. Bao and S. L. Gilat, *Acc. Chem. Res.*, 2001, **34**, 359.

2 J. Locklin, M. E. Roberts, S. C. B. Mannsfeld and Z. Bao, *Polym. Rev.*, 2006, **46**, 79.

3 J. Chisaka, M. Lu, S. Nagamatsu, M.C., Y. Yoshida, M. Goto, R. Azumi, M. Yamashita and K. Yase, *Chem. Mater.*, 2007, **19**, 2694.

4 (*a*) K. Ito, T. Suzuki, Y. Sakamoto, D. Kubota, Y. Inoue, F. Sato and S. Tokito, *Angew. Chem.*, 2003, **115**, 1191; (*b*) S. F. Nelson, Y.-Y. Lin, D. J. Gundlach and T. N. Jackson, *Appl. Phys. Lett.*, 1998, **72**, 1854; (*c*) A. Afzali, C. D. Dimitrakopoulos and T. C. Breen, *J. Am. Chem. Soc.*, 2002, **124**, 8812; (*d*) D. J. Gundlach, J. A. Nichols, L. Zhou and T. N. Jackson, *Appl. Phys. Lett.*, 2002, **80**, 2925; (*e*) H. Klauk, M. Halik, U. Zschieschang, G. Schmid and W. Radlik, *J. Appl. Phys.*, 2002, **92**, 5259.

5 (*a*) A. Dodabalapur, L. Torsi and H. E. Katz, *Science*, 1995, **268**, 270; (*b*) R. Hajlaoui, D. Fichou, G. Horowitz, B. Nessakh, M. Constant and F. Garnier, *Adv. Mater.*, 1997, **9**, 557; (*c*) M. Halik, H. Klauk, U. Zschieschang, G. Schmid, S. Ponomarenko, S. Kirchmeyer and W. Weber, *Adv. Mater.*, 2003, **15**, 917; (*d*) A. Facchetti, M. Mushrush, M.-H. Yoon, G. R. Hutchison, M. A. Ratner and T. J. Marks, *J. Am. Chem. Soc.*, 2004, **126**, 13859; (*e*) H. Meng, J. Zheng, A. J. Lovinger, B.-C. Wang, P. G. Van Patten and Z. Bao, *Chem. Mater.*, 2003, **15**, 1778; (*f*) Y. Miyata, M. Terayama, T. Minari, T. Nishinaga, T. Nemoto, S. Isoda and K. Komatsu, *Chem.–Asian J.*, 2007, **2**, 1492; (*g*) S. A. Ponomarenko, S. Kirchmeyer, A. Elschner, N. M. Alpatova, M. Halik, H. Klauk, U. Zschieschang and G. Schmid, *Chem. Mater.*, 2006, **18**, 579.

6 (*a*) D. Fichou, Ed. *Handbook of Oligo- and Polythiophenes*; Wiley-VCH: New York, 1999; (*b*) X. Zhang, M. Kőhler and A. J. Matzger, *Macromolecules*, 2004, **37**, 6306; (*c*) I. McCulloch, M. Heeney, C. Bailey, K. Genevicius, I. MacDonald, M. Shkunov, D. Sparrowe, S. Tieryney, R. Wagner, W. Zhang, M. L. Chabinyc, R. J. Kline, M. D. McGehee and M. F. Toney, *Nat. Mater.*, 2006, **5**, 328; (*d*) Y. Li, Y. Wu, P. Liu, M. Birau, H. Pan and B. S. Ong, *Adv. Mater.*, 2006, **18**, 3029; (*e*) E. Lim, B.-J. Jung, H.-K. Shim, T. Taguchi, B. Noda, T. Kambayashi, T. Mori, K. Ishikawa, H. Takezoe and L.-M. Do, *Org. Electron.*, 2006, **7**, 121; (*f*) L. S. Miguel and A. J. Matzger, *Macromolecules*, 2007, **40**, 9233; (*g*) E. Lim, B. J. Jung, J. Lee, H. K. Shim, J. I. Lee, Y. S. Yang and L. M. Do, *Macromolecules*, 2005, **38**, 4531.

7 (*a*) H. Meng, F. Sun, M. B. Goldfinger, G. D. Jaycox, Z. Li, W. J. Marshall and G. S. Blackman, *J. Am. Chem. Soc.*, 2005, **127**, 2406; (*b*) J. A. Merlo, C. R. Newman, C. P. Gerlach, T. W. Kelley, D. V. Muyres, S. E. Frits, M. F. Toney and C. D. Frisbie, *J. Am. Chem. Soc.*, 2005, **127**, 3997; (*c*) K. Xiao, Y. Liu, T. Qi, W. Zhang, F. Wang, J. Gao, W. Qiu, Y. Ma, G. Cui, S. Chen, X. Zhan, G. Yu, J. Qin, W. Hu and D. Zhu, *J. Am. Chem. Soc.*, 2005, **127**, 13281.

8 (*a*) H. Meng, F. Sun, M. B. Goldfinger, G. D. Jaycox, Z. Li, W. J. Marshall and G. S. Blackman, *J. Am. Chem. Soc.*, 2005, **127**, 2406; (*b*) D. R. Rutherford, J. K. Stille, C. M. Elliott and V. R. Reichert, *Macromolecules*, 1992, **25**, 781.

9 (*a*) F. Garnier, A. Yassar, R. Hajlaoui, G. Horowitz, F. Deloffre, B. Servet, S. Ries and P. Alnot, *J. Am. Chem. Soc.*, 1993, **115**, 8716; (*b*) A. Facchetti, Y. Deng, A. C. Wang, Y. Koide, H. Sirringhaus, T. J. Marks and R. H. Friend, *Angew. Chem., Int. Ed.*, 2000, **39**, 4547.

10 (*a*) M. L. Tang, T. Okamoto and Z. Bao, *J. Am. Chem. Soc.*, 2006, **128**, 16002; (*b*) M. L. Tang, M. E. Roberts, J. J. Locklin, M. M. Ling, H. Meng and Z. Bao, *Chem. Mater.*, 2006, **18**, 6250.

11 (*a*) M. O. Ahmed, C. Wang, P. Keg, W. Pisula, Y.-M. Lam, B. S. Ong, S.-C. Ng, Z.-K. Chen and S. G. Mhaisalkar, *J. Mater. Chem.*, 2009, **19**, 3449; (*b*) H.-S. Kim, Y.-H. Kim, T.-H. Kim, Y.-Y. Noh, S. Pyo, M. H. Yi, D.-Y. Kim and S.-K. Kwon, *Chem. Mater.*, 2007, **19**, 3561.

12 Y. Y. Noh, R. Azumi, M. Goto, B. J. Jung, E. Lim, H. K. Shim, Y. Yoshida, K. Yase and D. Y. Kim, *Chem. Mater.*, 2005, **17**, 3861.

13 J. G. Laquindanum, H. E. Katz, A. J. Lovinger and A. Dodabalapur, *Adv. Mater.*, 1997, **9**, 36.

14 C. Videlot-Ackermann, J. Ackermann, H. Brisset, K. Kawamura, N. Yoshimoto, P. Raynal, A. El Kassmi and F. Fages, *J. Am. Chem. Soc.*, 2005, **127**, 16346.

15 (*a*) W. Tang, L. Ke, L. Tan, T. Lin, T. Kietzke and Z.-K. Chen, *Macromolecules*, 2007, **40**, 6164; (*b*) L. Ke, W. Tang, Y. Song, Z.-K. Chen and S. J. Chua, *J. Appl. Phys.*, 2007, **102**, 063103.

16 W. Tang, T. Lin, L. Ke and Z.-K. Chen, *J. Polym. Sci., Part A: Polym. Chem.*, 2008, **46**, 7725.

17 (*a*) W. Tang, T. Kietzke, P. Vemulamada and Z.-K. Chen, *J. Polym. Sci., Part A: Polym. Chem.*, 2007, **45**, 5266; (*b*) W. Tang, L. Ke and Z.-K. Chen, *J. Phys. Chem. B*, 2008, **112**, 3590; (*c*) W. Tang, V. Chellappan, M. Liu, Z.-K. Chen and L. Ke, *ACS Appl. Mater. Interfaces*, 2009, **1**, 1467.

18 (*a*) A. Facchetti, M. Mushrush, M.-H. Yoon, G. R. Hutchison, M. A. Ratner and T. J. Marks, *J. Am. Chem. Soc.*, 2004, **126**, 13859; (*b*) F. Garnier, R. Hajlaoui, A. El Kassmi, G. Horowitz, L. Laigre, W. Porzio, M. Armanini and F. Provasoli, *Chem. Mater.*, 1998, **10**, 3334.

19 L. S. Fuller, B. Iddon and K. A. Smith, *J. Chem. Soc., Perkin Trans. 1*, 1997, 3465.

20 D. M. de Leeuw, M. M. J. Simenon, A. R. Brown and R. E. F. Einerhand, *Synth. Met.*, 1997, **87**, 53.

21 H. E. Katz and Z. Bao, *J. Phys. Chem. B*, 2000, **104**, 671.

22 (*a*) H. Sirringhaus, N. Tessler and R. H. Friend, *Science*, 1998, **280**, 1741; (*b*) H. E. Katz, A. J. Lovinger, J. Johnson, C. Kloc, T. Siegrist, W. Li, Y. Y. Lin and A. Dodabalapur, *Nature*, 2000, **404**, 478.

23 (*a*) R. Ruiz, D. Choudhary, B. Nickel, T. Toccoli, K.-C. Chang, A. C. Mayer, P. Clancy, J. M. Blakely, R. L. Headrick, S. Iannotta and G. G. Malliaras, *Chem. Mater.*, 2004, **16**, 4497; (*b*) D. G. de Oteyza, E. Barrena, S. Sellner, J. O. Ossó and H. Dosch, *Surf. Sci.*, 2007, **601**, 4117.

24 P. Sonar, S. P. Singh, S. Sudhakar, A. Dodabalapur and A. Sellinger, *Chem. Mater.*, 2008, **20**, 3184.